Biochimica et Biophysica Acta 1814 (2011) 1120–1126

Contents lists available at ScienceDirect

Biochimica et Biophysica Acta

journal homepage: www.elsevier.com/locate/bbapap

Structural stability of *Staphylococcus xylosus* lipase is modulated by Zn^{2+} ions

Jean Borges Bertoldo [a], Guilherme Razzera [a], Javier Vernal [a], Fábio Cristiano Angonesi Brod [b], Ana Carolina Maisonnave Arisi [b], Hernán Terenzi [a,*]

[a] Centro de Biologia Molecular Estrutural, Departamento de Bioquímica, Centro de Ciências Biológicas, Universidade Federal de Santa Catarina, Campus Trindade, 88040-900, Florianópolis, SC, Brazil
[b] Departmento de Ciência e Tecnologia de Alimentos, Universidade Federal de Santa Catarina, 88040900 Florianópolis, SC, Brazil

ARTICLE INFO

Article history:
Received 19 November 2010
Received in revised form 19 April 2011
Accepted 25 April 2011
Available online 19 May 2011

Keywords:
Metallolipase
Circular dichroism
Thermal stability
Thermostable lipase

ABSTRACT

Lipases are well-known enzymes extensively used in industrial biotransformation processes. Besides, their structural and catalytic characteristics have attracted increasing attention of several industries in the last years. In this work, we used biophysical and molecular modeling tools to assess structural properties of *Staphylococcus xylosus* lipase (SXL). We studied the thermal unfolding of this protein and its zinc-dependent thermotolerance. We demonstrated that SXL is able to be active and stable at moderate temperatures, but this feature is only acquired in the presence of Zn^{2+}. Such characteristic indicates SXL as a zinc-dependent metallolipase.

1. Introduction

Lipids constitute a large part of the earth's biomass, and lipolytic enzymes play an important role in the turnover of these water insoluble compounds [1–3]. The hydrolysis of fat is the primary reaction of lipases and lipolytic enzymes are involved in breakdown and thus in the mobilization of lipids within cells of individual organism as well as in the transfer of lipids from one organism to another [3]. Lipases usually exhibit a good chemioselectivity, regioselectivity, enantioselectivity and possess a broad substrate specificity exhibiting optimum activities over a wide range of temperatures [1,4]. Lipases also catalyze esterification, transesterification, acydolysis, alcoholysis and aminolysis in addition to the hydrolytic activity on triglycerides [4–6]. Structurally most lipases are included in the α/β-hydrolase fold, which is characterized by five to eight β-strands connected by α-helices to form an α/β/α sandwich. In most family members the β-strands are parallel [7]. Typically lipases present a catalytic triad including a serine residue located inside the conserved region Gly-X-Ser-X-Gly, as well as a histidine residue, which interacts with an aspartate or glutamate residue [8]. Moreover, in most lipases, an amphipathic flexible helical lid-domain, which covers the active site, is supposed to mediate substrate binding [9].

The production of lipases is a general property of staphylococci. These lipases are expressed as pre-pro-enzymes and have molecular masses of approximately 70 kDa. After secretion into the medium, proteolytic processing generates the 40–46 kDa mature lipase form. Many staphylococcal lipases were purified and characterized biochemically [6,10–13]. It seems that the mature forms of these lipases present high homology, with identities ranging from 48 to 99%.

Staphylococcus xylosus is a bacterium commonly found in fermented meat products. *Staphylococcus* strains are known for ensuring color stability, preventing lipid oxidation and producing aromatic compounds due to their lipolytic and proteolytic activities [14]. Several staphylococcal lipases were purified and characterized biochemically [6,10,13].

There are two lipases described for *S. xylosus*. One was reported by Mosbah et al. [10] and the other one, similar to AF208229, was recently characterized by our group [13,15]. The SXL is a moderately thermostable enzyme that presents high similarity with other staphylococcal lipases and with substrate specificity for short-chain lipids and higher activity on neutral to alkaline pH, and moderate temperature conditions [13]. It has been reported that some lipases present metal binding domains and the divalent ions are frequently found in coordinating sites on the overall structure of these enzymes [9,16–19]. Most bacterial lipases bind Ca^{2+} ions and may play a crucial role in the stabilization of the three-dimensional structure. As an example, in the lipase from *Burkholderia glumae* it was demonstrated that calcium influences thermal stability [19,20]. It was also described that Zn^{2+} may be involved in structural stability, but its correlation with catalytic function, mainly in staphylococcal lipases remains poorly understood [9,16,17,45]. In this work, we used biophysical and molecular modeling tools to assess structural properties of *S. xylosus* lipase SXL. We studied the thermal unfolding of this protein and its zinc-dependent thermotolerance and activity. We demonstrate that SXL thermal stability is modulated by Zn^{2+} ions.

* Corresponding author. Tel.: +55 48 3721 6426.
E-mail address: hterenzi@ccb.ufsc.br (H. Terenzi).

1570-9639
doi:10.1016/j.bbapap.2011.04.020

2. Materials and methods

2.1. Structural modeling

The bioinformatics analysis of the SXL was done using the following tools. Multiple sequence alignment was performed using the ClustalW algorithm [21]. The amino acid sequences were compared with the non-redundant sequence databases deposited at the NCBI (National Center for Biotechnology Information, USA) using the BLAST algorithm [22]. The molecular modeling was carried out using the software Swiss PDB Viewer [23] based on 2HIH PDB structure from *Staphylococcus hyicus*. The 2HIH structure was the best hit found using BLAST analysis against Protein Data Bank with 56% identity and was also automatically selected by the Swiss Modeler [23–25]. The zinc and calcium binding sites were energy minimized using Gromos96 force field implemented in Swiss PDB viewer. All structural quality checks were obtained by Swiss Modeler and also upon manual inspections of the Ramachandran plot. The final figure of SXL 3D model was obtained by PyMOL [26].

2.2. Cloning, expression and purification

Escherichia coli strain DH5α was used as a host for gene cloning and plasmid propagation, and strain BL21 (DE3) pLysS for protein expression. HisTrap affinity column connected to an ÄKTA HPLC system (GE Healthcare) was used for purification as described previously [13]. After purification a stock solution of the recombinant lipase (3 mg/ml) was incubated with 100 μM $ZnSO_4$ for reconstitution for 1 h at 37 °C (described as holoSXL).

2.3. Production of apoSXL

After purification a second solution of the recombinant lipase (1.75 mg/ml) was dialyzed against a buffer (50 mM NaH_2PO_4, 300 mM NaCl, pH 8.0) containing 10 mM EDTA at 8 °C for 48 h using a dialysis membrane D92277 (Sigma-Aldrich, Saint Louis, USA). EDTA is a recognized chelator with high specificity for divalent ions. Thus, in a second step the same protein solution was dialyzed in the same buffer without EDTA to prevent its effects on enzymatic and structural assays. In this step protein was named 'apoSXL.' For reconstitution, apoSXL solution was incubated with 100 μM $ZnSO_4$ or 100 μM $CaCl_2$ for 1 h at 37 °C, and named 'apoSXLrec' (rec = reconstituted).

2.4. Activity measurements

The lipase activity was measured spectrophotometrically at 20 °C, 25 °C, 37 °C, 42 °C, 50 °C, 60 °C or 70 °C after an optimization of the activity measurement protocol combining the best reaction conditions as previously established by us [13]. Production of *p*-nitrophenol as a result of *p*-nitrophenyl-butyrate hydrolysis was continuously monitored at 410 nm for 3 min in a final volume of 300 μl, using a spectrophotometer equipped with a Peltier temperature control unit (Amersham Ultrospec Pro 2100). HoloSXL, apoSXL and apoSXLrec were concentrated to 10 μM and used to assay lipolytic activity. One unit of lipase was defined as the amount of enzyme that released 1 nmol of *p*-nitrophenol per minute.

2.5. Structural analysis

The three forms of SXL were dialyzed against buffer (20 mM NaH_2PO_4, 20 mM NaCl, pH 7.4). The spectroscopic analysis was performed in a JASCO J-815 spectropolarimeter equipped with a Peltier temperature control unit and a fluorescence detection unit. The measurements of circular dichroism was carried out in a 0.2 cm pathlength cuvette (50 nm/min scan speed, response time 2 s, band width 2 nm, data pitch 0.1 nm/s) with an average of 5 scans for each spectrum in a wavelength range from 195 nm to 280 nm. The CD signal at 222 nm was also used as standard for calculations of secondary structures [27]. The measurements of fluorescence was carried out in 1 cm cuvette using 295 nm as excitation wavelength and scanning the fluorescence emission over the range from 300 nm to 400 nm.

2.5.1. Melting experiments

The thermal unfolding accompanied by circular dichroism was performed by increasing the temperature of the cuvette, containing the holo, apo and reconstituted apo forms with metals separately, from 10 °C to 70 °C. Spectra were collected following temperature increases (slope of 2.5 °C/min). The calculations were performed according to Eq. 1 followed by Eq. 2:

$$f_u = ([\theta]_{222} - [\theta]_N) / ([\theta]_U - [\theta]_N) \quad [17] \tag{1}$$

where $[\theta]_{222}$ is the mean residue molar ellipticity at 222 nm wavelength expressed as (degree cm^2 $dmol^{-1}$) and provided by Eq. 2 and $[\theta]_N$ and $[\theta]_U$ are the mean residue molar ellipticities of the native and denaturated states, respectively.

$$[\theta] = (\theta \times 100 \times M) / (C \times l \times n) \tag{2}$$

where θ is the ellipticity in degrees, l is the optical path in cm, C is the concentration of sample in mg/ml, M is the molecular mass and n is the number of residues in the protein.

3. Results and discussion

3.1. SXL sequence and 3D model analysis

A comparison of SXL amino acid sequence with non-redundant sequence databases was performed using the BLAST algorithm, and a multiple alignment was performed using ClustalW [22]. Fig. 1 shows the alignment against other lipases with reported crystallographic structures. The first one is the best hit found in PDB from *S. hyicus* and shares high identity (56%) with SXL. The second one, from *Bacillus stearothermophilus*, is an example of the lower identity sequences group found using BLAST analysis (39% identity).

The catalytic site is totally conserved between several sequences analyzed. Most staphylococcal lipases are homologues showing high similarity, and these proteins diverged from a common ancestor into a number of hydrolytic enzymes with a wide range of substrate specificities, together with other proteins with no recognized catalytic activity. In addition, the catalytic triad of SXL is located in loops, one of which, the nucleophile elbow, is the most conserved feature of the fold and occurs in most members of this family [28–30].

Particularly in the lipase from *S. hyicus*, the residues Lys295, Glu292, Thr294 and Ser356 are important for the phospholipid activity and the Lys residue has hydrogen bond interactions with the phospholipid [9]. In SXL the Lys and Glu positions are occupied by Phe residues that are not able to form the hydrogen bond network reported in the *S. hyicus* structure. This is an interesting feature of SXL and these aromatic residues may influence the ligand binding and specificity.

The structural model built for SXL (Fig. 2A), using the best hit PDB *S. hyicus* lipase (2HIH) as a template, shows two conserved metal binding sites. One of them is suggested to bind zinc ion, coordinated by the residues Asp63, His83, His89, and Asp235 (Fig. 2B). These residues are highly conserved between the reported lipase structures from *S. hyicus* and *B. stearothermophilus*, and are located far from the catalytic triad Ser115, His345, Asp306 ruling out the direct involvement of zinc on the lipolytic activity. According to previous crystallographic studies [9,16], the other metal coordination site binds calcium, and probably this site is also present in SXL lipase involving the residues

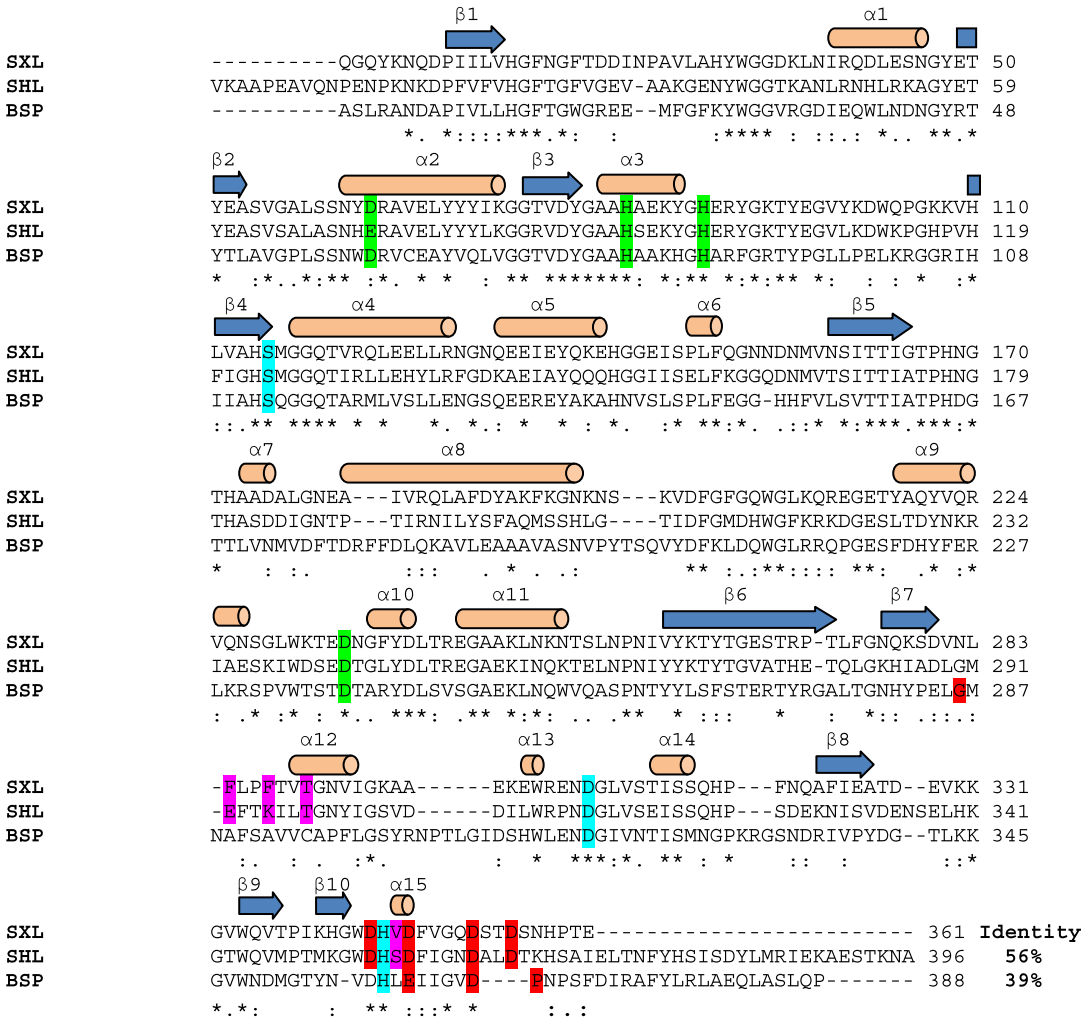

Fig. 1. Sequence alignment of *Staphylococcus xylosus* lipase (SXL) against homologous lipases SHL (2HIH) from *Staphylococcus hyicus* and BSP (1JI3) from *Bacillus stearothermophilus*. In highlighted blue, the residues from the catalytic triad; in green, residues responsible for zinc ion coordination, and in red, those involved in calcium coordination. In magenta, the residue positions reported to be responsible for the hydrogen bond network with phospholipids in SHL [9]. The secondary structure elements predicted for SXL are presented above the sequences and the identity level obtained by Blastp analysis is shown. The alignment was generated by Clustal 2.1 software [21].

Asp344, Asp347, Asp352 and Asp355. Furthermore, in several bacterial lipases the calcium binding site is structurally conserved, even in other genera as in *B. glumae* which calcium coordinates Asp241, Asp287, Gln291 and Val297 [20]. Nevertheless, the calcium binding site may occupy different positions. An example is the BSP (1JI3) from *B. / INS; stearothermophilus*, which involves the residues Glu360, Gly286, Pro366 and Asp365 (Fig. 1). It is important to note that the calcium binding site is most probably located at the C-terminus of SXL, but frequently the N- and C-terminal regions of proteins are more flexible and may avoid, in this case, the possibility of stable calcium coordination. In SHL, which binds calcium, the C-terminus of the protein has an α-helix [9] that may be important for the stabilization of the calcium site. Our results suggest that calcium does not influence the structure stability of SXL.

3.2. The holo and apo SXL lipolytic activity

Although there are some reports on biochemical characterization of *S. xylosus* lipases [6,10,12,14] little is known about how metal ions affect their structural and enzymatic properties. In this work we describe how zinc ions can modulate the structure of the *S. xylosus* lipase SXL. The *S. xylosus* lipase presents a maximum activity of 54.61 U mg^{-1} at 50 °C (Fig. 3). However, we observe activity even at higher temperatures (60 °C and 70 °C). These results were obtained after Zn^{2+} supplementation of the purified enzyme, which provided a 5.5-fold enhancement of lipolytic activity at 42 °C, when compared to our previous work [13]. Additionally, the holoSXL form after Zn^{2+} treatment is also capable to refold and retain full activity after 15 min incubation at 95 °C (Supplementary fig. S1). The lipase from *S. xylosus* (AF701336), described by Mosbah et al. [10,11,31], presented an optimal activity at 45 °C and was able to maintain only 50% of its activity after 15 min incubation at 60 °C. To evaluate the contribution of metal ions on lipase activity we performed experiments with the apo form of SXL. The holo form was dialyzed against a buffer containing EDTA and then recovered in the presence of zinc ions. It was evident that the apoform of SXL (apoSXL) exhibited a drastic reduction on activity, compared to the holoSXL. It is important to note that at lower temperature (20 °C) the activity is equivalent between the holo, apo, and apo treated with Zn (apoSXLrec) indicating that Zn^{2+} is important to stabilize the SXL fold at higher temperatures, but does not influence the catalytic activity directly.

Many biotechnological processes require the presence in the reaction media of certain ions that could act as modifiers of the enzyme activity, and metalloenzymes or metal tolerant proteins play

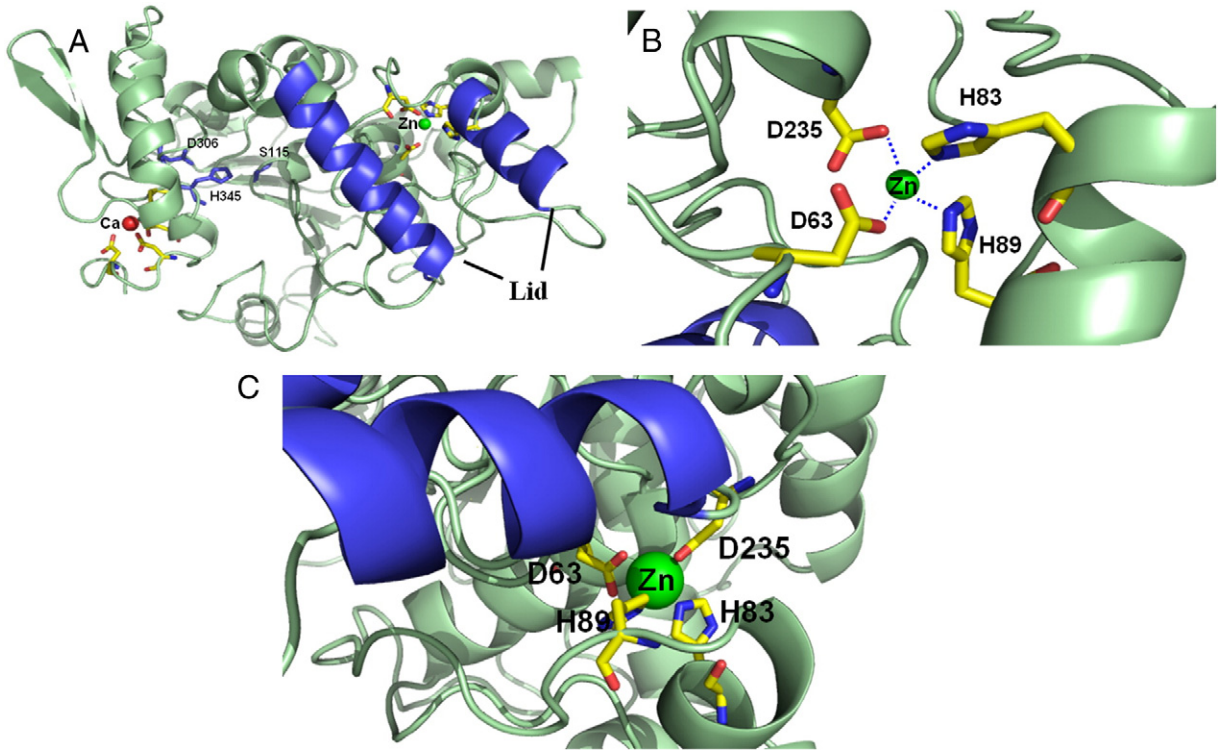

Fig. 2. Structural model of lipase SXL built against 2HIH PDB. In panel A, the overall aspects of α/β lipase monomer fold with the helices predicted to form the lid domain (in blue) in the open conformation. The two metal binding sites for zinc (in green) and calcium (in red) were identified in the SXL structural model and the catalytic triad amino acids were colored in blue. In panel B, a close-up view of zinc-coordination environment is shown in stick representation involving the residues His83, His89, Asp235 and Asp63. The figure was generated using PyMOL (http://www.pymol.org).

an important role in biocatalytic processes [32]. Several lipases have been reported to be stimulated by Zn^{2+} ions [33–38] as well as inhibited [39–42]. Moreover, it has been suggested that the effect of metal ions could be attributed to a change in the solubility and behavior of the substrate and also to a change in the catalytic properties of the enzyme itself [43]. In contrast, in *S. xylosus* lipase, there is no evidence of Zn^{2+} ion involvement in the catalytic process, and indeed, the SXL structural model shows that Zn^{2+} ion and the catalytic residues are separated by at least 18.8 Å, a distance that may preclude a direct effect of Zn^{2+} in the catalytic pocket of SXL.

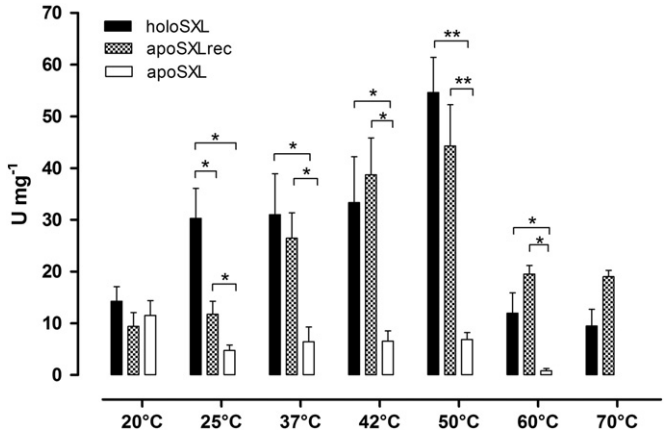

Fig. 3. Enzymatic activity of SXL assayed at different temperatures and conditions. Activity assay was carried out with 500 μM *p*-nitrophenyl-butyrate as substrate in 50 mM Tris–HCl buffer (pH 8.0) using protein concentrated to 10 μM. HoloSXL: *Staphylococcus xylosus* lipase after affinity purification, apoSXL: *S. xylosus* lipase in the presence of 10 mM EDTA, apoSXLrec: *S. xylosus* lipase reconstituted with 100 μM $ZnSO_4$ for 1 h at 37 °C after EDTA treatment. Results are expressed as mean ± SE of 3 independent experiments, (*) $p \leq 0.05$, (**) $p \leq 0.01$.

3.3. The Zn^{2+} ion is involved on structural stability

In order to investigate influence of metal ions on the structure of SXL, we performed experiments using CD and fluorescence analyses in the presence and absence of Zn^{2+} and Ca^{2+} metal ions. As previously described [13,15] SXL exhibits a typical α-helical secondary structure profile with minimal peaks at 208 nm and 222 nm [27]. The deconvoluted spectrum obtained by CDSSTR analysis [44] with the holoSXL suggests a mix content of α-helical (37%) and β-sheet (21%) secondary structures, in agreement with proteins belonging to the α/β-hydrolase fold [7], and with the SXL model (30% α-helices and 16% β-sheets; Fig. 2).

We evaluated the effect of Zn^{2+} on the overall structure of SXL through CD and fluorescence analyses at 20 °C, 25 °C, 37 °C, 42 °C, and 50 °C. Fig. 4A shows the circular dichroism analysis, and we note that holoSXL does not display large changes in the overall structure from 15 °C to 42 °C when compared with the apoSXL, where a disordered spectra is clearly detected [27] at 42 °C (Fig. 4B). Interestingly, when we analyze the secondary structural content of the apo-form, we calculated 10% less α-helices even at lower temperatures, which indicates that the metal ions are important for the SXL fold. The fluorescence data at 20 or 25 °C also agrees with a less structured protein in the apo form (see Supplementary fig. 2A) with a red shift of tryptophan maximum emission from 336 to 344 nm, and higher emission intensity in the apoSXL. Tryptophan residues are distributed throughout the protein, and as observed in Fig. 1, Trp208 is at 5.7 Å from the Zn^{2+} ion (Supplementary fig. 2B). In this sense, the average of the fluorescence signal may reflect the solvent exposure of Trp residues observed in the apo form, and may also be correlated to the Trp208 contribution. We can hypothesize that the presence of Zn^{2+}

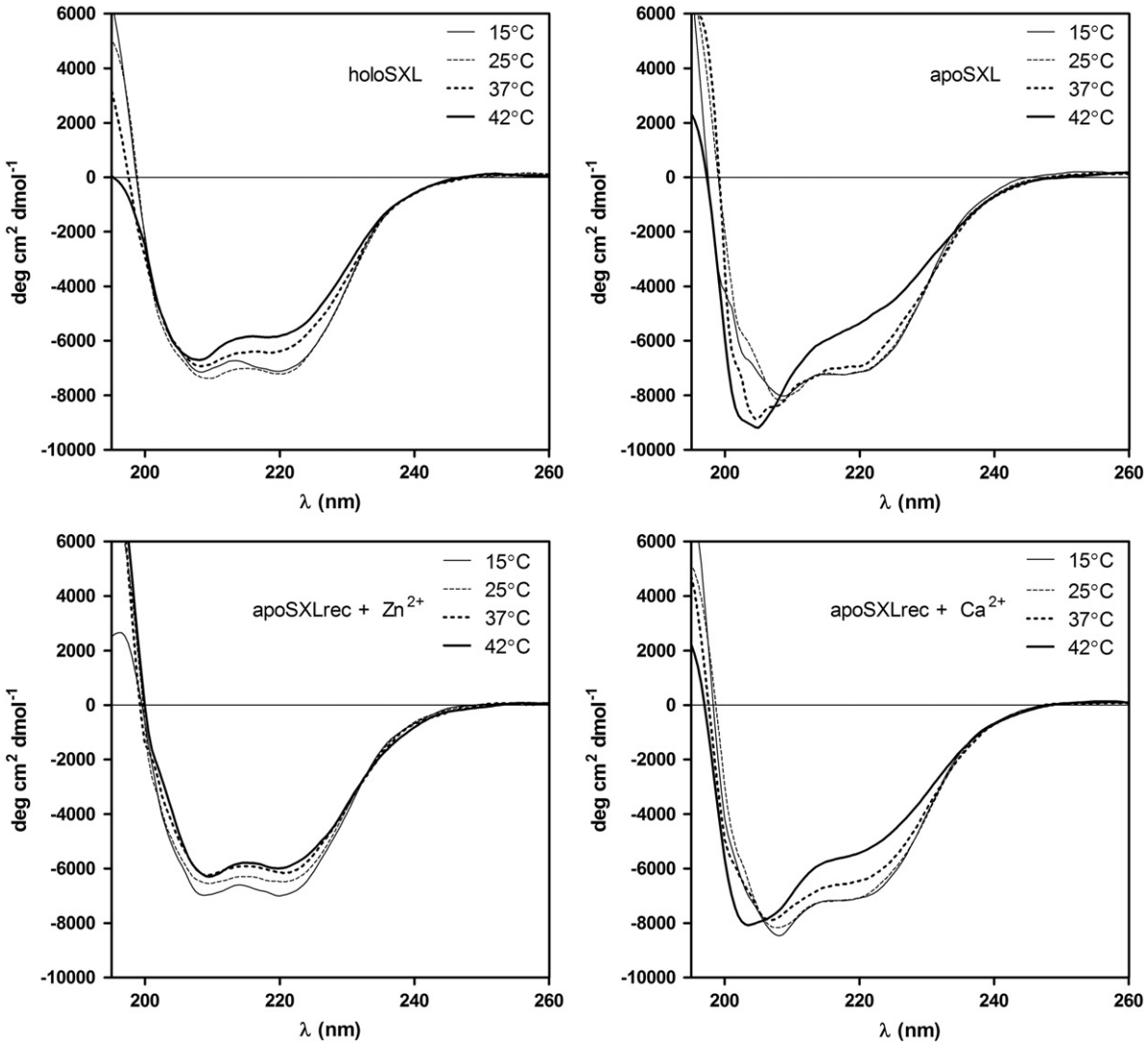

Fig. 4. Circular dichroism of holo and apo *Staphylococcus xylosus* lipase at different temperatures and metal conditions. The proteins were concentrated to 4 μM in buffer containing 20 mM NaH_2PO_4, 20 mM NaCl, pH 8.0. The apoform of SXL was reconstituted with 100 μM $ZnSO_4$ (apoSXLrec + Zn^{2+}) or 100 μM $CaCl_2$ (apoSXLrec + Ca^{2+}). The spectra were acquired in a 0.2 cm pathlength cuvette at continuous speed scanning (50 nm/min) using a JASCO J815 spectropolarimeter equipped with a Peltier temperature control unit. The overall spectra represent the average of five scans per sample per temperature.

ion may stabilize the helices 2 and 3 (see Fig. 1), where the coordinating residues D63 and H83 are respectively located, and this may contribute to the higher α-helical content of the holoSXL. These helices probably are also less affected during the unfolding process of the holo form.

The CD spectra obtained for apoSXLrec (Fig. 4C) revealed a similar behavior to that of holoSXL with minimal peaks at 208 nm and 222 nm very consistent with the observed recovery of the enzyme activity and structure upon Zn^{2+} addition. On the other hand, the apoSXL supplemented with Ca^{2+} presents a different behavior, with a disordered structure at 42 °C similar to the apoSXL (Fig. 4D). These results were further confirmed by fluorescence analyses. The fluorescence spectra obtained for apoSXL (Fig. 5B) agree with its CD spectra (dotted line), since it was observed a significant shift on maximum emission spectra of tryptophans (352 nm) suggesting a quite drastic structural change, which increased the solvent exposure of tryptophans. After Zn^{2+} addition (Fig. 5C) the red shift of maximum emission spectra of tryptophans, previously observed for apoSXL, was not detected in apoSXLrec, and the obtained spectra were similar to holoSXL (Fig. 5A).

In addition, the SXL T_m value was analyzed by CD monitoring the 222 nm peak over temperature. The T_m for apoSXL (Fig. 6, squares) was 11.0 °C lower than that detected for holoSXL (51.9 °C) indicating that the apoSXL is more susceptible to thermal denaturation. After apoSXL reconstitution with Zn^{2+} (Fig. 6, circles), the susceptibility to temperature diminished, and the T_m value for apoSXLrec was similar to holoSXL (55.2 °C). However, upon Ca^{2+} addition to apoSXL, the T_m value was 43.5 °C, which suggests that only Zn^{2+} is responsible for the fold stability at higher temperatures, although we could not rule out the possibility that Ca2+ ions are not accessible to EDTA, as reported previously [20]. As observed in the crystal structure of *S. hyicus* lipase, the Zn^{2+}- and Ca^{2+}-binding domains are present. In this case the metal ions are important for structural stabilization and activity maintenance [9]. Carrasco-López et al. [18] also described that these ions contribute for the secondary elements flexibility in the tertiary structure of the protein, promoting specific H-bonds interactions and rearrangements which promote the more stable active state at higher temperatures. In *Geobacillus stearothermophilus* lipase, which also contains a zinc binding site, the metal ion is also implicated in thermal stability at elevated temperatures. This thermophilic protein presents

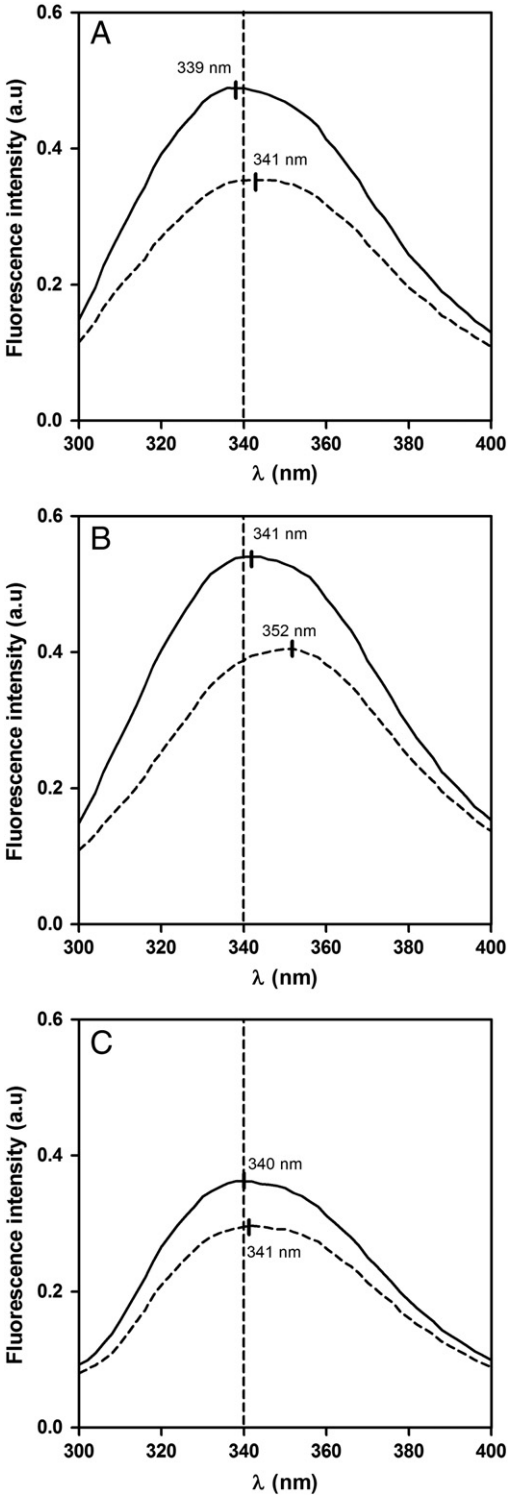

Fig. 5. Fluorescence spectra of *Staphylococcus xylosus* lipase. (Panel A) holoSXL; solid line 37 °C, dashed line 50 °C. (Panel B) apoSXL; solid line 37 °C, dashed line 50 °C. (Panel C) apoSXLrec; solid line 37 °C, dashed line 50 °C. Spectra were collected in a 1-cm pathlength quartz cuvette using an excitation wavelength of 295 nm and protein concentrated to 10 μM.

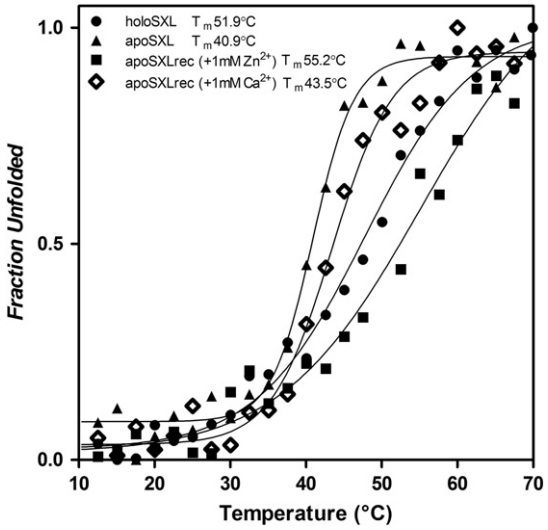

Fig. 6. Boltzmann sigmoidal plot of thermal unfolding of *Staphylococcus xylosus* lipase. The decrease in circular dichroism signal at 222 nm was measured. Data points were collected over a slope of 2.5 °C/min.

optimum catalytic activity at 60 °C and the addition of Zn^{2+} to the enzyme elevates the T_m value from 51.1 to 69.3 °C [17]. In SXL the addition of calcium ions to the apo-form does not affect the protein thermal resistance. This may be due to the fact that SXL does not bind Ca^{2+} or it is also possible that the Ca^{2+} binding site has no influence in the SXL structural folding. In another lipase from *S. xylosus* described by Mosbah et al. [10], Ca^{2+} was not required to trigger the activity when using tributyrin or emulsified olive oil as substrate.

Taken together, these results underline the need of the divalent cation Zn^{2+} for structural stability of SXL. Although some reports highlighted the structural role of Zn^{2+} and its involvement on lipase activity, the Zn^{2+} ion in SXL seems to be involved only in its structural stability. As described by Karjiban et al. [45] one specific feature of any lipase is the shielding of its catalytic site by a lid controlling the access of the substrate. In *B. stearothermophilus* lipase L1 the movement of the lid domain seems required to adopt an active conformation and the zinc-coordinated domain appears to control the lipase activation through interactions with the loop connected to the helical lid [45]. Such behavior is also found in *Staphylococcus simulans* lipase. By stabilizing some specific helix, the zinc ion therefore seems to be involved in the enzyme stability and activity. Furthermore, the region of the zinc-binding site makes tight contacts with a long loop between helical elements that are extended from the C-terminus of the putative lid helix [46]. In addition, these tight interactions at the C-terminus are also involved in thermostability of several lipases including *Staphylococcal* lipases [47].

In the SXL model we suggest the presence of two helices which form the lid for the ligand (see Fig. 2) reported in the SHL structure (2HIH) [9]. The residue Asp235, which coordinates Zn^{2+} ion is located in a loop close to the lid helix 9. Taking this into account, we might speculate that at higher temperatures, the Zn^{2+} ion could be involved in the maintenance of the lid helices in an adequate position for the ligand accessibility. Further experiments will be necessary to clarify the importance of Zn^{2+} on SXL lipase activity; indeed our results are important evidences indicating Zn^{2+} as a cofactor necessary for the proper folding and stability of the enzyme.

4. Conclusion

These results are the first insight on structural characterization of *S. xylosus* lipase and reveal the involvement of Zn^{2+} ion in the structural stability of this enzyme. These data also demonstrate that SXL is a moderate thermostable lipase showing residual activities over a wide range of temperatures. Besides, its thermostable profile is strongly zinc-dependent and may be interesting in an industrial environment.

Supplementary materials related to this article can be found online at doi: 10.1016/j.bbapap.2011.04.020.

Acknowledgments

The present work was supported by CNPq #552508/2007-1, Rede Proteoma de Santa Catarina (FAPESC/FINEP/MCT), and CAPES.

References

[1] A. Pandey, S. Benjamin, C.R. Soccol, P. Nigam, N. Krieger, V.T. Soccol, The realm of microbial lipases in biotechnology, Biotechnol. Appl. Biochem. 29 (1999) 119–131.
[2] B. Joseph, P.W. Ramteke, G. Thomas, Cold active microbial lipases: some hot issues and recent developments, Biotechnol. Adv. 26 (2008) 457–470.
[3] F. Beisson, A. Tiss, C. Rivière, R. Verger, Methods for lipase detection and assay: a critical review, Eur. J. Lipid Sci. Technol. 102 (2000) 133–153.
[4] P. Fojan, P.H. Jonson, M.T.N. Petersen, S.B. Petersen, What distinguishes an esterase from a lipase: a novel structural approach, Biochimie 82 (2000) 1033–1041.
[5] F. Carriere, K. Thirstrup, S. Hjorth, E. Boel, Cloning of the classical guinea pig pancreatic lipase and comparison with the lipase related protein 2, FEBS Lett. 338 (1994) 63–68.
[6] R. Rosenstein, F. Götz, Staphylococcal lipases: biochemical and molecular characterization, Biochimie 82 (2000) 1005–1014.
[7] T. Hotelier, L. Renault, X. Cousin, V. Negre, P. Marchot, A. Chatonnet, ESTHER, the database of the α/β-hydrolase fold superfamily of proteins, Nucleic Acids Res. 32 (2004) D145–D147.
[8] K.E. Jaeger, B.W. Dijkstra, M.T. Reetz, Annual Review of Microbiology, 53, 1999, pp. 315–351.
[9] J.J.W. Tiesinga, G.v. Pouderoyen, M. Nardini, S. Ransac, B.W. Dijkstra, Structural basis of phospholipase activity of *Staphylococcus hyicus* lipase, J. Mol. Biol. 371 (2007) 447–456.
[10] H. Mosbah, A. Sayari, H. Mejdoub, H. Dhouib, Y. Gargouri, Biochemical and molecular characterization of *Staphylococcus xylosus* lipase, Biochimica et Biophysica Acta - General Subjects 1723 (2005) 282–291.
[11] H. Mosbah, A. Sayari, S. Bezzine, Y. Gargouri, Expression, purification, and characterization of His-tagged *Staphylococcus xylosus* lipase wild-type and its mutant Asp 290 Ala, Protein Expression Purif. 47 (2006) 516–523.
[12] H. Horchani, H. Mosbah, N.B. Salem, Y. Gargouri, A. Sayari, Biochemical and molecular characterisation of a thermoactive, alkaline and detergent-stable lipase from a newly isolated *Staphylococcus aureus* strain, J. Mol. Catal. B: Enzym. 56 (2009) 237–245.
[13] F.C.A. Brod, M.R. Pelisser, J.B. Bertoldo, J. Vernal, C. Bloch Jr., H. Terenzi, A.C.M. Arisi, Heterologous expression and purification of a heat-tolerant *Staphylococcus xylosus* lipase, Mol. Biotechnol. 44 (2010) 110–119.
[14] C.B. Spricigo, P.B. Pianovsky, Effect of the use of curing salts and of a starter culture on the sensory and microbiological characteristics of homemade salamis, Brazilian Archives of Biology and Technology 48 (2005) 169–174.
[15] D.J. Kolling, J.B. Bertoldo, F.C.A. Brod, J. Vernal, H. Terenzi, A.C.M. Arisi, Biochemical and structural characterization of two site-directed mutants of *Staphylococcus xylosus* lipase, Mol. Biotechnol. (2010) 1–8.
[16] J.D.A. Tyndall, S. Sinchaikul, L.A. Fothergill-Gilmore, P. Taylor, M.D. Walkinshaw, Crystal structure of a thermostable lipase from *Bacillus stearothermophilus* P1, J. Mol. Biol. 323 (2002) 859–869.
[17] W.C. Choi, H.K. Myung, H.S. Ro, R.R. Sang, T.K. Oh, J.K. Lee, Zinc in lipase L1 from *Geobacillus stearothermophilus* L1 and structural implications on thermal stability, FEBS Lett. 579 (2005) 3461–3466.
[18] C. Carrasco-López, C. Godoy, B. de las Rivas, G. Fernández-Lorente, J.M. Palomo, J.M. Guisán, R. Fernández-Lafuente, M. Martínez-Ripoll, J.A. Hermoso, Activation of bacterial thermo alkalophilic lipases is spurred by dramatic structural rearrangements, J. Biol. Chem. 284 (2009) 4365–4372.
[19] G. Invernizzi, E. Papaleo, R. Grandori, L. De Gioia, M. Lotti, Relevance of metal ions for lipase stability: structural rearrangements induced in the *Burkholderia glumae* lipase by calcium depletion, J. Struct. Biol. 168 (2009) 562–570.
[20] E. Papaleo, G. Invernizzi, Conformational plasticity of the calcium-binding pocket in the *Burkholderia glumae* lipase: remodeling induced by mutation of calcium coordinating residues, Biopolymers 95 (2011) 117–126.
[21] J.D. Thompson, D.G. Higgins, T.J. Gibson, CLUSTAL W: improving the sensitivity of progressive multiple sequence alignment through sequence weighting, position-specific gap penalties and weight matrix choice, Nucleic Acids Res. 22 (1994) 4673–4680.
[22] S.F. Altschul, J.C. Wootton, E.M. Gertz, R. Agarwala, A. Morgulis, A.A. Schäffer, Y.K. Yu, Protein database searches using compositionally adjusted substitution matrices, FEBS J. 272 (2005) 5101–5109.
[23] N. Guex, M.C. Peitsch, SWISS-MODEL and the Swiss-PdbViewer: an environment for comparative protein modeling, Electrophoresis 18 (1997) 2714–2723.
[24] T. Schwede, J. Kopp, N. Guex, M.C. Peitsch, SWISS-MODEL: an automated protein homology-modeling server, Nucl. Acids Res. 31 (2003) 3381–3385.
[25] K. Arnold, L. Bordoli, J. Kopp, T. Schwede, The SWISS-MODEL workspace: a web-based environment for protein structure homology modelling, Bioinformatics 22 (2006) 195–201.
[26] A.T. Brünger, P.D. Adams, G.M. Clore, W.L. Delano, P. Gros, R.W. Grossekunstleve, J.S. Jiang, J. Kuszewski, M. Nilges, N.S. Pannu, R.J. Read, L.M. Rice, T. Simonson, G.L. Warren, Crystallography & NMR system: a new software suite for macromolecular structure determination, Acta Crystallogr. Sect. D. Biol. Crystallogr. 54 (1998) 905–921.
[27] S.M. Kelly, T.J. Jess, N.C. Price, How to study proteins by circular dichroism, Biochim. et Biophys. Acta - Proteins and Proteomics 1751 (2005) 119–139.
[28] D.L. Ollis, E. Cheah, M. Cygler, B. Dijkstra, F. Frolow, S.M. Franken, M. Harel, S.J. Remington, I. Silman, J. Schrag, J.L. Sussman, K.H.G. Verschueren, A. Goldman, The α/β hydrolase fold, Protein Eng. 5 (1992) 197–211.
[29] L. Brady, A.M. Brzozowski, Z.S. Derewenda, E. Dodson, G. Dodson, S. Tolley, J.P. Turkenburg, L. Christiansen, B. Huge-Jensen, L. Norskov, L. Thim, U. Menge, A serine protease triad forms the catalytic centre of a triacylglycerol lipase, Nature 343 (1990) 767–770.
[30] M. Holmquist, Alpha/beta-hydrolase fold enzymes: structures, Functions and Mechanisms, Current Protein and Peptide Science 1 (2000) 209–235.
[31] H. Mosbah, A. Sayari, H. Horchani, Y. Gargouri, Involvement of Gly 311 residue on substrate discrimination, pH and temperature dependency of recombinant *Staphylococcus xylosus* lipase: a study with emulsified substrate, Protein Expression Purif. 55 (2007) 31–39.
[32] C. Bofill, N. Prim, M. Mormeneo, A. Manresa, F.I. Javier Pastor, P. Diaz, Differential behaviour of *Pseudomonas* sp. 42A2 LipC, a lipase showing greater versatility than its counterpart LipA, Biochimie 92 (2010) 307–316.
[33] B.S. Demir, S.S. Tükel, Purification and characterization of lipase from *Spirulina platensis*, J. Mol. Catal. B: Enzym. 64 (2010) 123–128.
[34] E.H. Ahmed, T. Raghavendra, D. Madamwar, A thermostable alkaline lipase from a local isolate *Bacillus subtilis* EH 37: characterization, partial purification, and application in organic synthesis, Appl. Biochem. Biotechnol. 160 (2010) 2102–2113.
[35] P. Esakkiraj, M. Rajkumarbharathi, A. Palavesam, G. Immanuel, Lipase production by *Staphylococcus epidermidis* CMST-Pi 1 isolated from the gut of shrimp *Penaeus indicus*, Annals of Microbiology 60 (2010) 37–42.
[36] S. Dutta, L. Ray, Production and characterization of an alkaline thermostable crude lipase from an isolated strain of *Bacillus cereus* C7, Appl. Biochem. Biotechnol. 159 (2009) 142–154.
[37] X. Wang, X. Yu, Y. Xu, Homologous expression, purification and characterization of a novel high-alkaline and thermal stable lipase from *Burkholderia cepacia* ATCC 25416, Enzyme Microb. Technol. 45 (2009) 94–102.
[38] S.L. Wang, Y.T. Lin, T.W. Liang, S.H. Chio, L.J. Ming, P.C. Wu, Purification and characterization of extracellular lipases from *Pseudomonas monteilii* TKU009 by the use of soybeans as the substrate, J. Ind. Microbiol. Biotechnol. 36 (2009) 65–73.
[39] R. Liu, X. Jiang, H. Mou, H. Guan, H. Hwang, X. Li, A novel low-temperature resistant alkaline lipase from a soda lake fungus strain *Fusarium solani* N4-2 for detergent formulation, Biochem. Eng. J. 46 (2009) 265–270.
[40] S. Cherif, Y. Gargouri, Thermoactivity and effects of organic solvents on digestive lipase from hepatopancreas of the green crab, Food Chem. 116 (2009) 82–86.
[41] V. Dandavate, J. Jinjala, H. Keharia, D. Madamwar, Production, partial purification and characterization of organic solvent tolerant lipase from *Burkholderia multivorans* V2 and its application for ester synthesis, Bioresour. Technol. 100 (2009) 3374–3381.
[42] K. Chakraborty, R.P. Raj, An extra-cellular alkaline metallolipase from *Bacillus licheniformis* MTCC 6824: purification and biochemical characterization, Food Chem. 109 (2008) 727–736.
[43] E. Lesuisse, K. Schanck, C. Colson, Purification and preliminary characterization of the extracellular lipase of *Bacillus subtilis* 168, an extremely basic pH-tolerant enzyme, Eur. J. Biochem. 216 (1993) 155–160.
[44] L. Whitmore, B.A. Wallace, DICHROWEB, an online server for protein secondary structure analyses from circular dichroism spectroscopic data, Nucleic Acids Res. 32 (2004) W668–W673.
[45] R. Abedi Karjiban, M.B. Abdul Rahman, M. Basri, A.B. Salleh, D. Jacobs, H. Abdul Wahab, Molecular dynamics study of the structure, flexibility and dynamics of thermostable L1 lipase at high temperatures, Protein J. 28 (2009) 14–23.
[46] F. Frikha, M. Ladjimi, Y. Gargouri, N. Miled, 3-D structure modelling of the *Staphylococcus simulans* lipase: conformational changes, substrate specificity and novel structural features, FEMS Microbiol. Lett. 286 (2008) 207–221.
[47] S.T. Jeong, H.K. Kim, S.J. Kim, S.W. Chi, J.G. Pan, T.K. Oh, S.E. Ryu, Novel zinc-binding center and a temperature switch in the *Bacillus stearothermophilus* L1 lipase, J. Biol. Chem. 277 (2002) 17041–17047.